

Introduction of a valence space in quasiparticle random-phase approximation: Impact on vibrational mass parameters and spectroscopic properties

F. Lechaftois,^{1,*} I. Deloncle,^{1,2} and S. Péru¹¹CEA, DAM, DIF F-91297 Arpajon, France²CSNSM, IN2P3/CNRS, F-91405 Orsay, France

(Received 27 November 2014; revised manuscript received 30 July 2015; published 15 September 2015)

For the first time, using a unique finite-range interaction (D1M Gogny force), a fully coherent and time-feasible calculation of the Bohr Hamiltonian vibrational mass is envisioned in a Hartree-Fock-Bogoliubov + quasiparticle random-phase approximation (QRPA) framework. In order to reach a reasonable computation time, we evaluate the feasibility of this method by considering two restrictions for the QRPA: the Tamm-Dancoff approximation and the insertion of a valence space. We validate our approach in the even-even tin isotopes by comparing the convergence scheme of the mass parameter with those of built-in QRPA outputs: excited-state energy and reduced transition probability. The seeming convergence of these intrinsic quantities is shown to be misleading and the difference with the theoretical expected value is quantified. This work is a primary step towards the systematic calculation of mass parameters.

DOI: [10.1103/PhysRevC.92.034315](https://doi.org/10.1103/PhysRevC.92.034315)

PACS number(s): 21.10.Re, 21.60.Ev, 21.60.Jz, 23.20.Lv

I. INTRODUCTION

One of the most challenging goals in nuclear physics is to describe all the nuclei of the chart using a unique formalism with as few free parameters as possible. Though very promising, the exact triaxial generator coordinate method (GCM) is for now unmanageable for heavy nuclei because of its outrageous computation cost [1–3]. Thus, the quadrupole 5-dimensional collective Hamiltonian (5DCH)—GCM under the Gaussian overlap approximation—is for now our only tool capable of dealing with both light (as soon as the concept of mean field is meaningful) and heavy nuclei under a common theoretical framework. Yet, several studies have already pointed out some drawbacks of this approach such as its inadequacy for describing rigid spherical nuclei, or more generally speaking, the dependence of the reliability of the results with the nuclear deformation [4,5]. Possible improvements would be to add beyond-mean-field correlations in mass parameters as suggested in Refs. [2,4–6]. The quasiparticle random-phase approximation (QRPA) could provide enriched microscopic ingredients entering the vibrational mass parameters to be used for the 5DCH Hamiltonian, if the computational burden is not too heavy. Since mass parameters exhibit strong variations with the deformation [7,8], they have to be computed for each point (β, γ) of a triaxial mesh. Such full QRPA calculations with the Gogny interaction are out of reach due to the calculation time needed for each (β, γ) point of the triaxial map. Some approximations, namely the finite amplitude method [9] or the Arnoldi diagonalization [10], have already been applied successfully to the RPA with zero-range interactions to obtain spectroscopic properties more rapidly. Local QRPA has led to satisfactory results in calculating mass parameters, first restricted to pairing plus quadrupole excitations [11], and more recently using the Skyrme interaction [12]. Here, we decide to test limitations of

the excitations (or correlations) to provide the first vibrational mass parameters obtained through QRPA with a Gogny interaction. Previous studies have already tested the impact of a cutoff of the 2-quasiparticle (2-qp) excitation energy in QRPA, such as Refs. [13] (Skyrme) and [14] (Gogny D1S), but the effect of an inert core in QRPA has never been considered. Approaches such as the one developed here, exploring ways of setting limitations inside the QRPA framework, are of high interest. By reducing the mass parameter computational time, it could open the path towards considerable improvement in the 5DCH approach. In this paper, we briefly consider the Tamm-Dancoff approximation (TDA), in which ground-state correlations are neglected. Then, following standard shell-model techniques, we examine another way of restricting the excitations that consists in introducing a valence space, i.e., limited excitation space, in QRPA calculations. The convergence of the mass parameter is discussed for the first time according to different inert cores as well as the limits in the 2-qp excitation energy that are set. The convergence of the QRPA excitation energies and reduced transition probabilities are examined at each step.

The present study is focused on ^{100–144}Sn (spherical) tin isotopes at zero deformation. It allows us to decorrelate the valence space from the deformation. This work evaluates the feasibility of the approach, and studies dedicated to the impact of the deformation and the effects of the new mass parameters on the 5DCH spectroscopy will be performed in the future.

II. FORMALISM

In a quadrupole 5DCH calculation, the seven parameters entering the Hamiltonian

$$H_{5DCH} = V + T_{\text{rot}} + T_{\text{vib}} \quad (1)$$

are obtained from constrained Hartree-Fock-Bogoliubov (CHFb) calculations over the (β, γ) map. These parameters are a collective potential V , three moments of inertia \mathcal{J}_i (with $i \in \{x, y, z\}$) for the rotational part, and three vibrational

*francois.lechaftois@cea.fr

mass parameters $B_{\mu\nu}$ (with $(\mu, \nu) \in \{0, 2\}^2$, $B_{02} = B_{20}$) for the vibrational part. These vibrational mass parameters can be obtained by using a formula analogous to the one derived in Ref. [15] for RPA

$$B_{\mu\nu} = \frac{\hbar^2}{2} \frac{\mathcal{M}_{-3, \mu\nu}}{[\mathcal{M}_{-1, \mu\nu}]^2}, \quad (2)$$

where the p th order moment $\mathcal{M}_{p, \mu\nu}$ of the quadrupolar strength distribution ($\hat{Q}_{2\nu}$) reads

$$\mathcal{M}_{p, \mu\nu} = \sum_n E_n^p |\langle \tilde{0} | \hat{Q}_{2\mu} | n \rangle \langle n | \hat{Q}_{2\nu} | \tilde{0} \rangle|. \quad (3)$$

When dealing with a HFB calculation, $|\tilde{0}\rangle$ is the vacuum for Bogoliubov quasiparticles as defined in Ref. [16] (later on, for the sake of simplicity, a Bogoliubov quasiparticle is merely called a quasiparticle, qp), $|n\rangle$ is a 2-qp excitation state, and E_n is the associated energy $E_n = E_{qp1} + E_{qp2}$. In the QRPA framework, $|\tilde{0}\rangle$ is the vacuum for QRPA excitations (phonons) and $|n\rangle$ is a QRPA phonon of energy ω_n defined by the quasiboson creation operator θ_n^+

$$\theta_n^+ |\tilde{0}\rangle = |n\rangle, \quad (4)$$

$$\text{with } \theta_n |\tilde{0}\rangle = 0 \quad (5)$$

$$\text{and } \theta_n^+ = \sum_{i < j} X_n^{ij} \eta_i^+ \eta_j^+ - Y_n^{ij} \eta_j \eta_i, \quad (6)$$

where i, j run over the qp levels obtained from the HFB ground state (spherical point for considered isotopes), $\eta^+(\eta)$ is the quasiparticle creation (annihilation) operator, and X_n, Y_n are the amplitudes of the 2-qp excitations. Following a few steps [17], Eq. (3) can be rewritten to work with mass parameters a la Thouless-Valatin:

$$\mathcal{M}_{p, \mu\nu} = \sum_n \omega_n^p |\langle \tilde{0} | \hat{Q}_{2\mu} \theta_n^+ | \tilde{0} \rangle \langle \tilde{0} | \hat{Q}_{2\nu} \theta_n^+ | \tilde{0} \rangle|. \quad (7)$$

The phonon energy ω_n is associated to the amplitudes X_n and Y_n which are solutions of the QRPA equation

$$\begin{pmatrix} A & B \\ B^* & A^* \end{pmatrix} \begin{pmatrix} X_n \\ Y_n \end{pmatrix} = \omega_n \begin{pmatrix} X_n \\ -Y_n \end{pmatrix}, \quad (8)$$

using the interaction matrices A and B.

We define

$$\hat{Q}_{20} = \sqrt{\frac{4\pi}{5}} r^2 Y_{20}, \quad (9)$$

$$\hat{Q}_{22} = \sqrt{\frac{4\pi}{5}} r^2 (Y_{22} + Y_{2-2}). \quad (10)$$

For spherical nuclei, it can be shown that

$$B_{00} = \frac{\hbar^2}{2} \frac{\mathcal{M}_{-3, 00}}{[\mathcal{M}_{-1, 00}]^2} = 2B_{20} = 4B_{22}. \quad (11)$$

This relation of proportionality allows us to restrict our study to B_{00} .

All calculations, at each step, are performed with the DIM Gogny force [18] in a harmonic oscillator basis with 11 major shells. It is worth noting that we checked the stability of the

results versus the number of major shells in the basis. The HFB calculations have been performed using the axial code of Ref. [19]. The full computation of the cylindrical QRPA [20] matrix elements of one nucleus requires approximately 2 000 CPU hours. It can now be spread over hundreds of MPI threads [14] to get the result within a day. We extract a submatrix from the QRPA matrix according to the desired valence space (depending on the approximation studied). We then diagonalize the matrix as explained in Ref. [20] and finally process the X_n and Y_n amplitudes with a fast portion of code in order to get the mass parameter and the energy spectrum with the corresponding γ strengths at once. It is worth noting that in the case of a full QRPA calculation, the potential spurious states go down to zero energy. For spherical nuclei, whatever the restriction considered, spurious states that would appear and not completely fall down to zero would still not be a problem. As a matter of fact, we study here $J = 2$ and $J = 3$ states only. Due to the sphericity, these states are fully decoupled from the possible spurious states, which can only be $J = 0$ or $J = 1$ states.

III. APPROXIMATIONS

A. Tamm-Dancoff approximation

Contrary to calculations based on the Skyrme interaction where the diagonalization is the most time-consuming part, filling the matrices A and B with the Gogny interaction is roughly 3 000 times longer than the diagonalization, and reducing the number of matrix elements is the most efficient way to decrease the computation load. The TDA assumes that there are no correlations in the ground state, except those coming from the HFB calculation. This implies that the interaction matrix B is null and results in $Y_n = 0$. Equation (8) then reduces to QTDA:

$$A X_n = \omega_n X_n, \quad (12)$$

which leads to a half-sized eigensystem problem and a calculation time divided by two. Figure 1(a) shows the

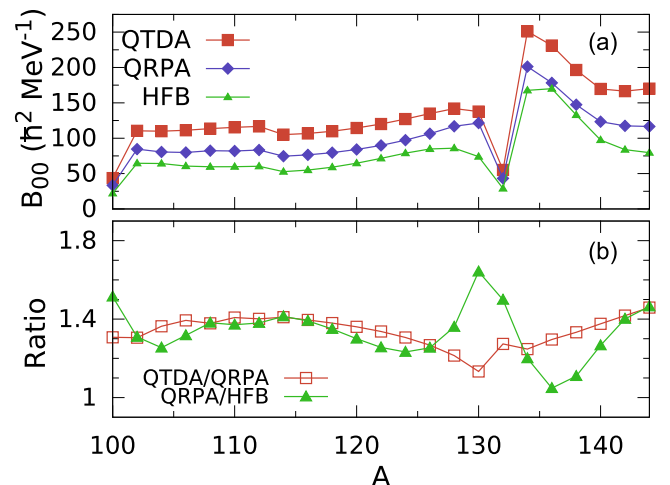


FIG. 1. (Color online) Variation of (a) B_{00}^{QTDA} , B_{00}^{QRPA} , B_{00}^{HFB} and (b) $B_{00}^{\text{QTDA}}/B_{00}^{\text{QRPA}}$, $B_{00}^{\text{QRPA}}/B_{00}^{\text{HFB}}$ with the mass number A.

evolution of the mass parameters calculated with QTDA, QRPA, and HFB for the whole isotopic chain. First, the HFB mass parameter exhibits a strong shell closure effect. Thus the mass parameter cannot be blamed for the inability of the 5DCH to deal with doubly magic nuclei. Second, the HFB mass parameters, known for being too low, are indeed lower than the QRPA ones. Figure 1(b) presents the variation with the mass number A of the $B_{00}^{\text{QTDA}}/B_{00}^{\text{QRPA}}$ and $B_{00}^{\text{QRPA}}/B_{00}^{\text{HFB}}$ ratios. It is worth noting that we obtain an average $B_{00}^{\text{QRPA}}/B_{00}^{\text{HFB}}$ ratio of 1.34 along the isotopic chain. This value is close to the average value of the range of factors usually applied to correct the HFB masses [21]. However, this ratio is anything but constant, in particular around $A = 130$. The peak in this region could be due to the fact that the QRPA brings even more correlations than HFB in the limit of low pairing, i.e., when the shell is nearly closed. Caution should then be taken when performing such a correction. Last but not least, the QTDA always overestimates the QRPA value by at least 15%, showing the great imprecision brought by this approximation. Although it dramatically reduces the computation time, the TDA is disqualified for mass parameter calculations and will then not be considered anymore. On a side note, we have performed some calculations for ^{110}Ru (oblate, $\beta \sim -0.2$) and ^{122}Xe (prolate, $\beta \sim 0.3$) in their ground states. The ratios $B_{00}^{\text{QRPA}}/B_{00}^{\text{HFB}}$ for these nuclei are respectively 0.727 and 2.17, which is still in the range of the aforementioned correction factor. Once, again, it shows that this ratio is not to be considered constant and that we will have to deal with the evolution of the factor along constrained deformation in the future.

B. Valence space

We now study the effect of the introduction of a valence space, i.e., a space in which the quasiparticles can be excited.

1. Cutoff on the 2-qp energy

The first limitation resulting from such a valence space is a restriction of the energy of the 2-qp excitations, viz., the sum of the two involved qp energies. Here we suppose that as the 2-qp excitation energy is higher, the importance in the nuclear response is lower, in the QRPA framework. A compromise should exist between a cutoff in 2-qp excitation energy and a reasonable mass parameter value. Figure 2 shows the evolution of B_{00} as a function of the cutoff for all tin isotopes. Cutoff values range between 10 and 100 MeV. Moreover, the QRPA no-cutoff value is considered as our reference calculation. We can first notice that except for some slight differences, all the isotopes behave similarly. Below 50 MeV, the mass parameters are ranging from 1.5 to 11 times higher than their respective converged values. For a cutoff of 50 MeV, we already have a fair approximation of the final mass parameters with less than 10% difference. This difference then shrinks to less than 5% at 80 MeV. If the purpose of the QRPA calculation is only to obtain mass parameters for the 5DCH, then it seems reasonable to use a 50-MeV cutoff. In this case, computation time is divided by a factor of 16 approximately. Whether we should consider 10% or 5% small enough is a question that

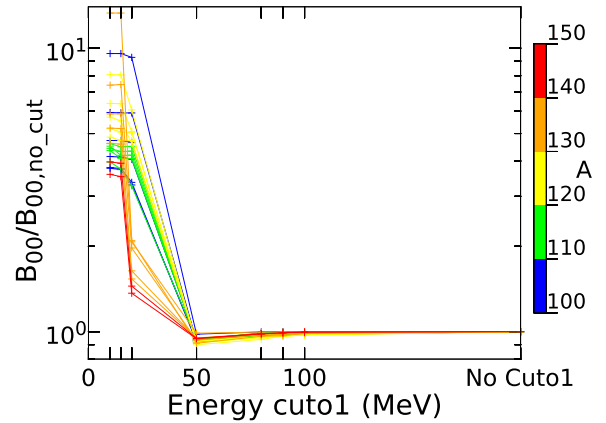


FIG. 2. (Color online) Convergence of B_{00} for $^{100-144}\text{Sn}$ with the cutoff. The results are normalized by the respective no-cutoff values.

would require a separate study evaluating the impact of such a difference on the results of the 5DCH. Due to the similarity of the behavior of the even-even tin isotopes mass parameters, the curves will be plotted for $^{112,120,124}\text{Sn}$ only in the following.

2. Inert core

In a full QRPA calculation, excitations of all nucleons, even the deepest ones, are taken into account. By imposing an inert core, we will only consider the excitations of the nucleons outside the core, those closer to the Fermi level. The nucleons located in the inert core are frozen and do not take part in the excitation process. The present study has been prepared with the following doubly magic cores: ^{40}Ca , ^{48}Ca , ^{56}Ni , ^{70}Ca , and ^{78}Ni (for ^{100}Sn , ^{70}Ca and ^{78}Ni cores are excluded for there would be no valence neutrons). Other doubly magic nuclei would be either too small and thus not sufficiently time-saving or too large to be used for at least one of the lightest tin isotopes.

The evolution of the mass parameter according to the inert core size (from ^{40}Ca to ^{78}Ni) as a function of the cutoff is presented in Fig. 3. Whatever the core is, the values are, as in Fig. 2, stabilized from a 50-MeV cutoff. On the one hand, the two lightest calcium cores give good (^{48}Ca) and even very good (^{40}Ca) approximated values. This can be seen in Fig. 3(d) since in Figs. 3(a)–3(c) their values are indistinguishable from the no-cutoff results. On the other hand, the last calcium (^{70}Ca) and the two nickel cores (^{56}Ni and ^{78}Ni) do not provide sufficiently good results. Therefore, choosing a $^{40,48}\text{Ca}$ core could be a wise choice for these isotopes, allowing us to obtain mass parameters 30% faster. We could even decide to use a 50-MeV cutoff in conjunction with a ^{40}Ca core to compute approximately 30 times faster acceptable mass parameters. However, we have to keep in mind that we praised the 5DCH for its ability to describe both light and heavy nuclei under a common framework, and we need to determine a coherent valence space—which is nucleus dependent—for different nuclei to be consistent.

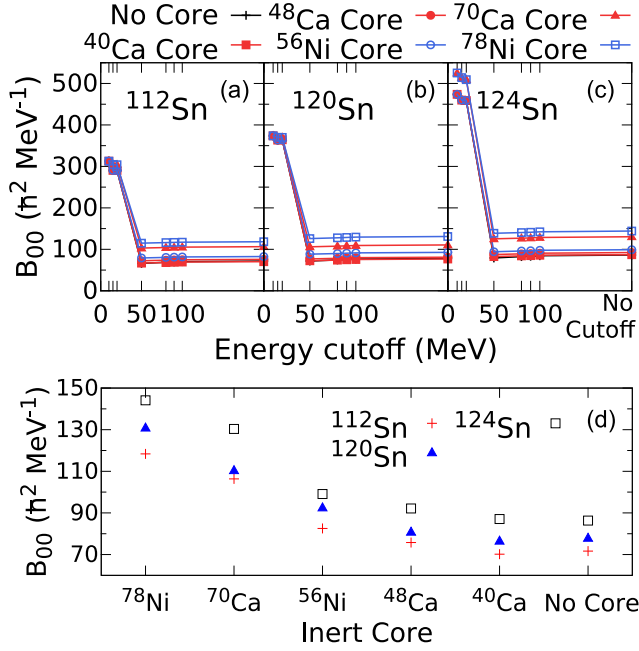


FIG. 3. (Color online) Evolution of B_{00} using Ca cores (filled points) and Ni cores (hollow points) as a function of the cutoff for (a) ^{112}Sn , (b) ^{120}Sn , and (c) ^{124}Sn . (d) Convergence with the core size without any cutoff.

IV. QRPA SPECTRA

Restricting the valence space appears to be an efficient way of saving computation time for the mass parameter calculation, but the robustness of this result and the underlying hypothesis, i.e., the low influence of the high-energy phonons in our mass parameter, have to be assessed. This can be achieved by examining the convergence scheme of QRPA intrinsic values such as the energy spectrum or the transition probabilities.

A. Cutoff on the 2-qp energy

Figure 4 shows the convergence of the 2_1^+ and 3_1^- energies and their reduced transition probabilities with the cutoff. The agreement between theoretical and experimental values of the 2_1^+ for tin isotopes can be found in Ref. [6] and will not be discussed here. Opposite trends are observed for the excited level energy and the associated transition probability of all the isotopes. Unlike mass parameters, the transition energies and probabilities do not reach convergence until a high-energy cutoff value. In order to reach the 10% difference, we need to extend our calculation up to 80 MeV and even 90 or 100 MeV for the 5% difference. For a 50-MeV 2-qp energy cutoff, the mass parameters are converged while the 2_1^+ and 3_1^- energies lie 30% away from the no-cutoff result. Mass parameters and QRPA phonon energies behave quite differently with respect to the 2-qp energy cutoff. Indeed, the high-energy 2-qp excitations appear not take an active part in mass parameters, when it is essential to get satisfactory phonon energies. In Fig. 4 we can also notice that the reduced transition probability is more sensitive to small energy cutoff values than the excited-state energy itself. Then the well-known

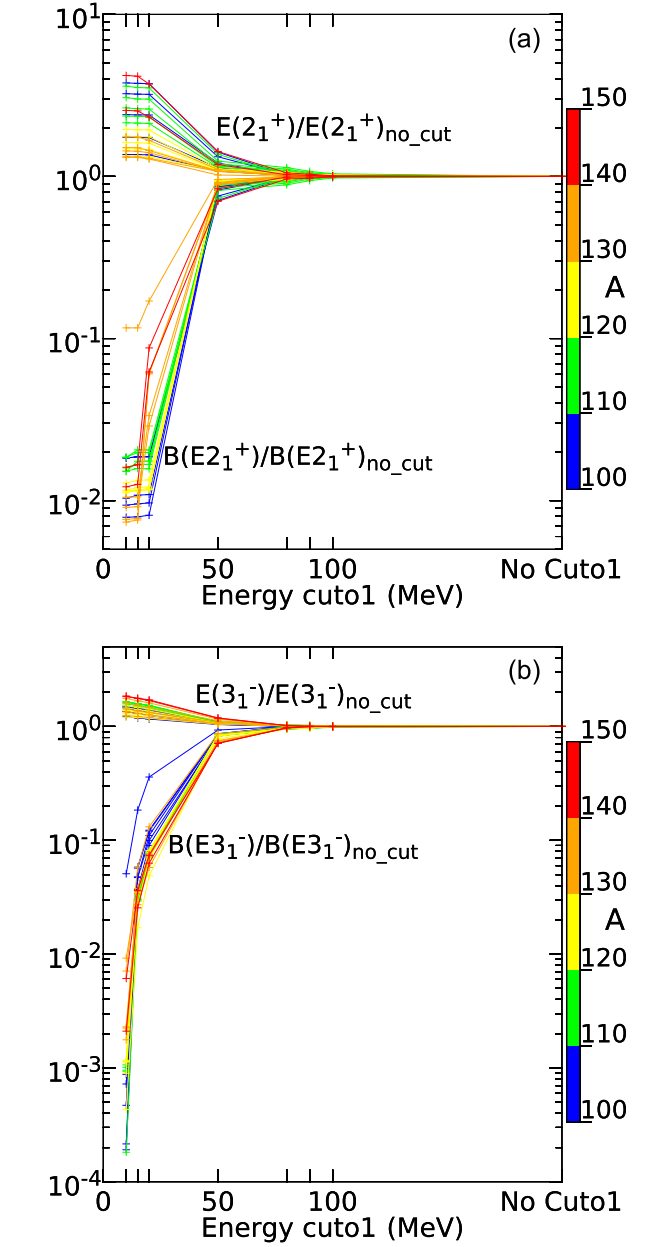


FIG. 4. (Color online) Relative variation of (a) $E(2_1^+)$, $B(E2_1^+, GS \rightarrow 2_1^+)$, $E(3_1^-)$ and (b) $E(3_1^-)$, $B(E3_1^-, GS \rightarrow 3_1^-)$ as a function of the cutoff for $^{100-144}\text{Sn}$.

relation [22]

$$E(2_1^+)B(E2_1^+) \propto ZA^{-1/3} \quad (13)$$

is violated for small-energy cutoff values.

B. Inert core

Let us now study the convergence of QRPA outputs as a function of the inert core size. We have performed calculations with different cores for $^{100-144}\text{Sn}$ but, as observed previously, they all follow a common trend and results for $^{112,120,124}\text{Sn}$ only are reported in Figs. 5 and 6. As for the cutoff study, transition energies and probabilities are much more sensitive

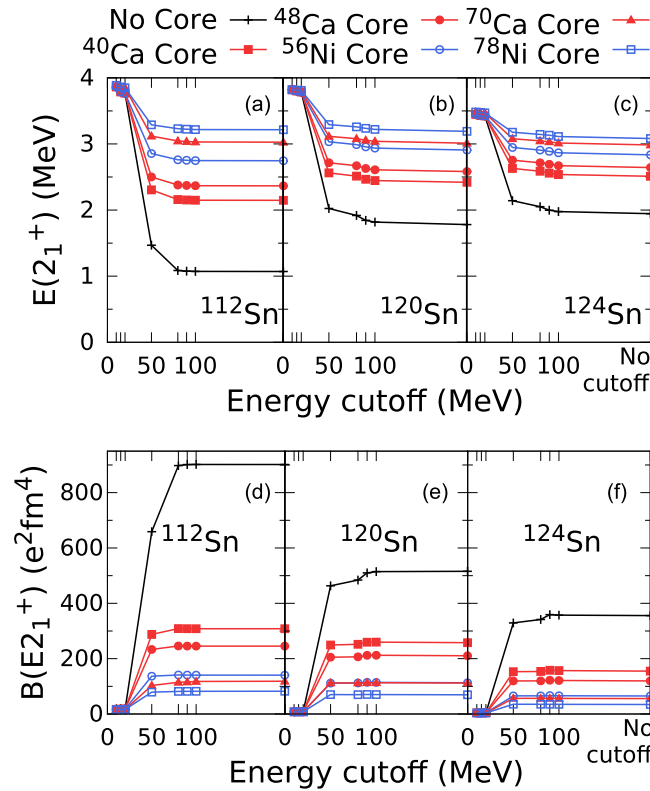


FIG. 5. (Color online) Evolution of $E(2_1^+)$ for (a) ^{112}Sn , (b) ^{120}Sn , (c) ^{124}Sn , and $B(E2_1^+, GS \rightarrow 2_1^+)$ for (d) ^{112}Sn , (e) ^{120}Sn , and (f) ^{124}Sn with the cutoff using different inert cores.

to the introduction of an inert core than mass parameters. None of the cores—even the smallest one of the set presented here—allows us to obtain a satisfying value. Indeed, ^{40}Ca -core calculation cannot reproduce the 2_1^+ properties, the transition probability is at least halved, and the energy is between 30 and 50% too high compared to the full-space calculation. Similar conclusions can be drawn for 3_1^- ; the eigenvalues (energy) converge more rapidly than the associated eigenvectors (X_n and Y_n used to build $B(E\lambda)$). It is worth noting that using an ^{16}O core, though clearly useless to reduce the computation time and thus not presented here, has proven to be extremely close to the no-core calculation.

By exhibiting the weak convergence properties of QRPA intrinsic quantities, this last study confirms the robustness of the QRPA mass parameter calculation with a valence space, including inert cores. Indeed, when imposing an inert core, one blocks high-energy qp excitations from deep qp levels, which play a weak role in the mass parameter value. On the contrary, they are found to play an important role in the excited-state energy and reduced transition probability. Consequently none of the inert cores can provide satisfying values of these quantities. Moreover, Fig. 5 demonstrates that whatever the inert core is, the evolution of $E(2_1^+)$ and $B(E2_1^+)$ as a function of the energy cutoff strongly resembles a convergence process. Nevertheless, this leads to values far from the expected no-core ones. Evaluating the product of $E(2_1^+)$ and $B(E2_1^+)$ could be helpful for choosing an appropriate valence space.

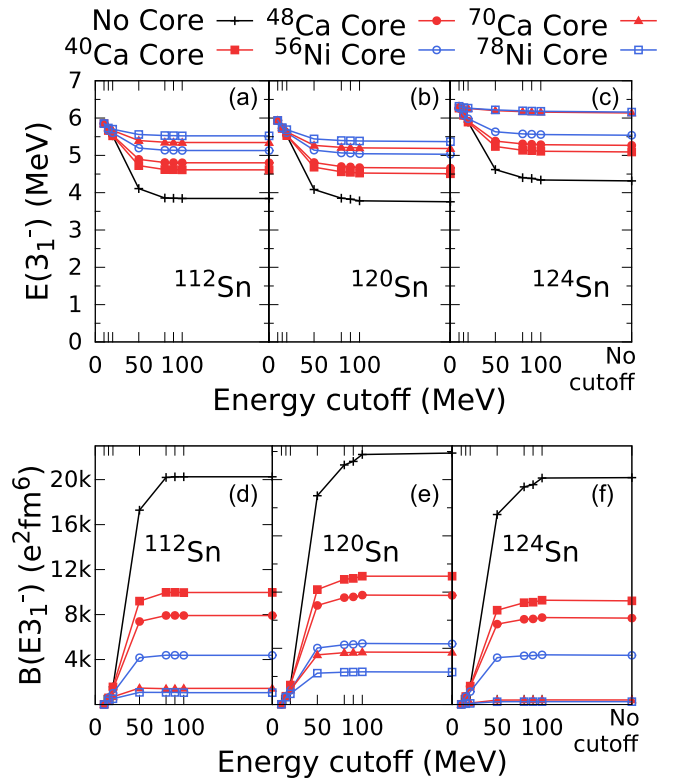


FIG. 6. (Color online) Evolution of $E(3_1^-)$ for (a) ^{112}Sn , (b) ^{120}Sn , (c) ^{124}Sn , and $B(E3_1^-, GS \rightarrow 3_1^-)$ for (d) ^{112}Sn , (e) ^{120}Sn , and (f) ^{124}Sn with the cutoff using different inert cores.

V. CONCLUSION

In this paper, we introduce a valence space for the calculation of even-even tin isotopes vibrational mass parameters in QRPA. The HFB 2-qp excitations entering the QRPA calculations are restricted by an energy cutoff and an inert core which define the valence space. This technique allows us to obtain vibrational mass parameters a la Thouless-Valatin, including more physics than those commonly used in the 5DCH approach. Indeed, using a valence space allows us to save computation time up to a factor of 30 compared to no-valence-space QRPA calculations. The rapidity of the convergence of the so-calculated mass parameter, as a function of the cutoff and the size of the inert core, is coherent with the fact that mass parameters do not require the inclusion of high-energy 2-qp excitations, in contrast with phonon energies; it validates our hypothesis. This convergence property leaves room for obtaining mass parameters in a reasonable computation time for deformed nuclei when the formalism is adapted to the case of constrained deformation far from the minimum of the potential energy surface. It would also allow us to face full (β, γ) mapping, when we are able to deal with triaxial systems in QRPA. The QRPA approach with a valence space that we are developing will contribute to broaden the amount of nuclear phenomena that can be described by the 5DCH, one of our most coherent and predictive tools for nuclear dynamics up to now.

Additionally, in this framework, we were able to show that phonon transition energies and reduced probabilities exhibit weak convergence properties. In particular, even with the small ^{40}Ca inert core, the 2_1^+ and 3_1^- energies are far from the no-core values. Thus in QRPA, caution should be taken when considering the calculation of intrinsic quantities (state energies, reduced transition probabilities) with a valence space. This result was expected as it is known that one should not use a universal effective interaction (like the Gogny force) when dealing with unreasonably small valence spaces. It is

worth noting that the convergence of intrinsic observables towards experimental values are of false appearance and thus misleading.

ACKNOWLEDGMENTS

F.L. acknowledges Marc Dupuis for his advice and the stimulating discussions while writing this paper and the DAM Ile-de-France for granting access to the TGCC supercomputers.

-
- [1] T. R. Rodríguez and J. L. Egido, *Phys. Rev. C* **81**, 064323 (2010).
 - [2] M. Bender and P.-H. Heenen, *Phys. Rev. C* **78**, 024309 (2008).
 - [3] B. Bally, B. Avez, M. Bender, and P. H. Heenen, *Phys. Rev. Lett.* **113**, 162501 (2014).
 - [4] J.-P. Delaroche, M. Girod, J. Libert, H. Goutte, S. Hilaire, S. Péru, N. Pillet, and G. F. Bertsch, *Phys. Rev. C* **81**, 014303 (2010).
 - [5] G. F. Bertsch, M. Girod, S. Hilaire, J.-P. Delaroche, H. Goutte, and S. Péru, *Phys. Rev. Lett.* **99**, 032502 (2007).
 - [6] S. Péru and M. Martini, *Eur. Phys. J. A* **50**, 88 (2014).
 - [7] B. Mohammed-Azizi, *Electronic J. Theor. Phys.* **9**, 143 (2012).
 - [8] E. Kh. Yuldashbaeva, J. Libert, P. Quentin, and M. Girod, *Phys. Lett. B* **461**, 1 (1999).
 - [9] T. Nakatsukasa, T. Inakura, and K. Yabana, *Phys. Rev. C* **76**, 024318 (2007).
 - [10] J. Toivanen, B. G. Carlsson, J. Dobaczewski, K. Mizuyama, R. R. Rodríguez-Guzmán, P. Toivanen, and P. Veselý, *Phys. Rev. C* **81**, 034312 (2010).
 - [11] N. Hinohara, K. Sato, T. Nakatsukasa, M. Matsuo, and K. Matsuyanagi, *Phys. Rev. C* **82**, 064313 (2010).
 - [12] K. Yoshida and N. Hinohara, *Phys. Rev. C* **83**, 061302 (2011).
 - [13] K. Yoshida and N. V. Giai, *Phys. Rev. C* **78**, 064316 (2008).
 - [14] S. Péru, G. Gosselin, M. Martini, M. Dupuis, S. Hilaire, and J.-C. Devaux, *Phys. Rev. C* **83**, 014314 (2011).
 - [15] D. Vautherin, *Phys. Lett. B* **69**, 393 (1977).
 - [16] N. N. Bogoliubov, *Nuovo Cimento* **7**, 794 (1958).
 - [17] M. K. Pal, D. Zawischa, and J. Speth, *Z. Phys. A* **272**, 387 (1975).
 - [18] S. Goriely, S. Hilaire, M. Girod, and S. Péru, *Phys. Rev. Lett.* **102**, 242501 (2009).
 - [19] S. Hilaire and M. Girod, *Eur. Phys. J. A* **33**, 237 (2007).
 - [20] S. Péru and H. Goutte, *Phys. Rev. C* **77**, 044313 (2008).
 - [21] J. Libert, J.-P. Delaroche, M. Girod, H. Goutte, S. Hilaire, S. Péru, N. Pillet, and G. F. Bertsch, *J. Phys.: Conf. Ser.* **205**, 012007 (2010).
 - [22] P. Ring and P. Schuck, *The Nuclear Many-Body Problem* (Springer-Verlag, New York, 1980), p. 15.